PHYSICAL REVIEW A **93**, 031402(R) (2016)

State-resolved three-dimensional electron-momentum correlation in nonsequential double ionization of benzene

Alexander H. Winney, Yun Fei Lin, Suk Kyoung Lee, Pradip Adhikari, and Wen Li*
Department of Chemistry, Wayne State University, Detroit, Michigan 48202, USA
(Received 11 September 2015; published 11 March 2016)

We report state-resolved electron-momentum correlation measurement of strong-field nonsequential double ionization in benzene. With a novel coincidence detection apparatus, highly efficient triple coincidence (electron-electron dication) and quadruple coincidence (electron-electron-cation-cation) are used to resolve the final ionic states and to characterize three-dimensional (3D) electron-momentum correlation. The primary states associated with dissociative and nondissociative dications are assigned. A 3D momentum anticorrelation is observed for the electrons in coincidence with dissociative benzene dication states whereas such a correlation is absent for nondissociative dication states.

DOI: 10.1103/PhysRevA.93.031402

Nonsequential double ionization (NSDI) is one of the most interesting and thoroughly studied strong-field phenomena. It is closely related to high harmonic generation and high-order above threshold ionization in the sense that *laser-induced recollision* plays a major role in all three processes. NSDI attracts particular interest because the ejection of two electrons requires a strong correlation between them, and thus it is an excellent benchmark system for modeling electron correlation in strongly driven multielectron atomic and molecular systems. Numerous experimental and theoretical studies have been carried out on NSDI (see a recent comprehensive review [1] and references therein), most of which focused on atomic systems. Among them, electron-momentum correlation measurements by cold target recoil ion momentum spectroscopy (COLTRIMS) provide the most direct information on electron correlation in NSDI. It has been shown that two electrons can be ejected either side by side or back to back parallel to the laser polarization depending on atomic species, laser intensity, and carrier envelop phase, etc. [2–7]. A few different NSDI mechanisms have been proposed based on experimental results: recollision-impact-ionization (RII) [8], recollision excitation and subsequent ionization (RESI) [3], and double delayed ejection involving doubly excited states [9,10]. It should be noted that the majority of these measurements were limited to one dimension, i.e., parallel to the laser polarization due to a limited momentum resolution in the other directions. Momentum correlation between two electrons has also been studied in a few simple diatomics, focusing on the structural effect (orbital structure and alignment dependence) [11,12]. An interesting question about NSDI remains unexplored: whether and how the three-dimensional (3D) electron-momentum correlation depends on the final dication states? This is an important question because NSDI is likely to produce different dication states due to a small energy gap between the ground state and the lowest excited states (typically <1 eV in many molecules). Furthermore, the ground states of dications are typically triplet states arising from losing two electrons with the same spin and thus from different orbitals. However, it has been calculated that triplet states are not favored in NSDI due to the Pauli exclusion principle [13] and some experimental evidence of this has been presented [14]. Therefore, it is important to resolve the final ionic state when measuring electron-momentum correlations to gain further insight into the electron correlation dynamics in NSDI. However, achieving such a capability is not a trivial task because there is no simple energy signature to help identify different cationic states, which is the underlying principle of photoelectron spectroscopy. This is partially due to the multiphoton nature of NSDI, e.g., the broad bandwidth of a femtosecond laser and the presence of Freeman resonance, etc. As a consequence, the energy spectra of NSDI are usually complex and cannot be simply used to identify dication states.

Here in this paper, we achieved a state-resolved electron-momentum correlation measurement of NSDI in benzene molecules. By detecting two electrons in coincidence with dications (triple coincidence) and fragments (quadruple coincidence), we observed different electron-momentum correlations. We assigned dication states by their different fates after double ionization (dissociative or nondissociative). We observed a 3D momentum anticorrelation in coincidence with dissociative benzene dications. Technically, because our coincidence imaging system featured minimized dead-time two-electron detection efficiency was greatly improved. Electron-electron coincidence measurements remove the requirement for a superb ion-momentum resolution in COLTRIMS experiments and enable electron-momentum correlation measurement to be applied to any atomic or molecular system. Meanwhile, 3D momenta of both electrons are readily available, which were rarely achieved in previous experiments.

The experiment was carried out in a velocity mapping coincidence apparatus, and the details will be reported elsewhere. Briefly, this apparatus features a six-electrode ion-electron optics that can velocity focus both ions and electrons to improve momentum resolution. A 30-fs 800-nm laser was focused onto the molecular beam by a spherical mirror mounted on a kinematic mirror mount in the vacuum. The estimated laser intensity was 1.2×10^{14} W cm^2. The laser polarization is along the time-of-flight (TOF) axis (Z axis). Benzene was bubbled into the chamber by helium carrier gas through a 20-μm diameter aperture, and the beam was double skimmed before entering the main chamber. The

*wli@chem.wayne.edu

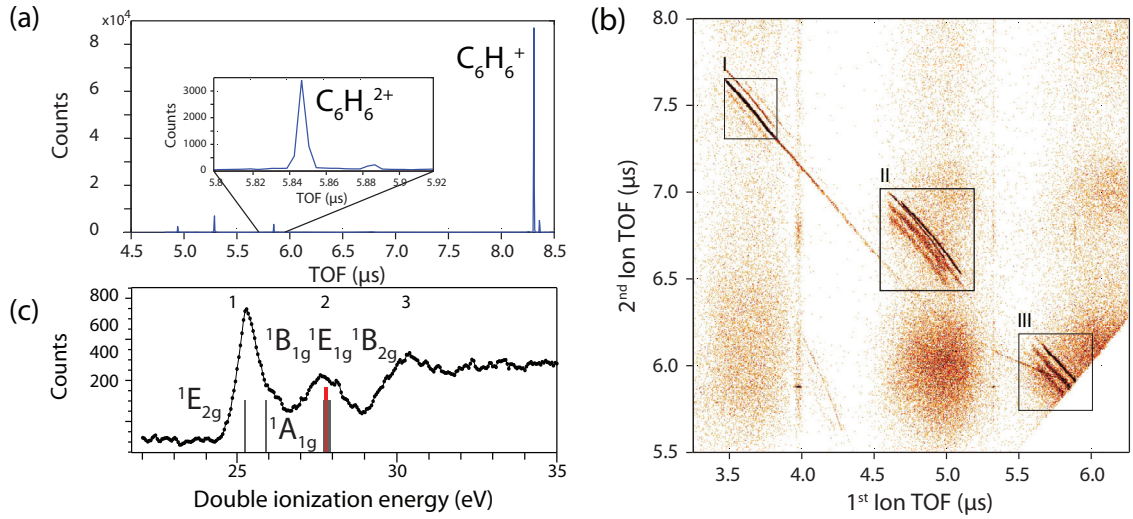

FIG. 1. (a) One-dimensional ion TOF of benzene strong-field ionization at 1.2×10^{14} W cm^2. The inset shows the mass peak of nondissociative benzene dication. (b) Two-dimensional ion TOF of benzene double ionization at the same laser intensity as (a). Areas I–III represent $CH_3^+ + C_5H_3^+$, $C_2H_3^+ + C_4H_3^+$, and $C_3H_3^+ + C_3H_3^+$ dissociation pathways, respectively, for dissociative benzene dications. Note in each area there are multiple dissociation pathways varied by a few protons in either fragment. However, the dominant pathways are as designated. (c) The single-photon double-ionization photoelectron spectrum, adapted from Fig. 1(a) of Ref. [19]. The positions of different states are from calculated values in Ref. [20] with a 1.3-eV shift in energy. The red marker represents the experimentally observed dissociation threshold (27.8 eV). It should be noted that the relative dication state population arising from NSDI could be different from that of single-photon double ionization due to the recollision mechanism involved in NSDI.

molecular-beam propagation direction (Y axis) was orthogonal to both the TOF axis (Z axis) and the laser propagation direction (X axis). The produced ions and electrons were then directed in opposite directions by an electric field and impacted on two microchannel-plate with phosphor screen (MCP-phosphor) imagers at the end of their TOF regions. The new MCP-phosphor-based 3D momentum imaging system has been described in detail elsewhere [15–17], and here we will only briefly reiterate the main points. This system is composed of three major components: a conventional MCP-phosphor screen imaging detector, a fast frame complementary metal-oxide semiconductor camera, and a high-speed digitizer. The camera and the high-speed digitizer are both triggered by the laser at 1 kHz. With correlated measurements between camera and digitizer, the position and arrival time of the single particle can be obtained. Multihit capability is achieved by correlating the brightness of camera pixels and the height of the MCP pulse measured by the digitizer [15]. The achieved electron time-of-flight resolution is better than 32 ps. With an advanced timing analysis algorithm, electron-electron detection dead time was reduced to less than 1 ns while a zero dead-time detection was also achieved [17]. This improvement has made the triple and quadruple coincidence detection highly efficient and is crucial for the current experiment. In this experiment, the count rate for electrons was about 0.1 per laser shot whereas that of ions was 0.07 per laser shot. We estimated the false coincidence rate to be less than 20%. To accumulate enough statistics, the overall data-acquisition time was about 180 h.

When benzene is subjected to a linearly polarized intense laser field, both single and double ionizations will take place while double ionization mainly proceeds through the NSDI mechanism at the intensity used in this study [18]. Dissociation will also occur on dication potential-energy surfaces if the states of benzene dications have enough energy to overcome the barrier. We will first look at the one-dimensional (1D) and two-dimensional (2D) ion TOF spectra showing in Figs. 1(a) and 1(b). It is evident the dominant ionization channel is single ionization whereas nondissociative dication only makes about ~4% of the overall ionization signal. The yield of dissociative channel is even lower. From the 2D ion TOF, three channels are observed for dissociative dications: $CH_3^+ + C_5H_3^+$,$C_2H_3^+ + C_4H_3^+$, and $C_3H_3^+ + C_3H_3^+$ in a descending order of yield. The 2D ion TOF spectrum is very similar to previous single-photon ionization studies. The measured kinetic-energy release of $CH_3^+ + C_5H_3^+$ is around 3.1 eV, which also matches well with previous works [21,22]. These suggest the current experiment is accessing similar dication states of benzene through NSDI as in single-photon ionization process. Because the $CH_3^+ + C_5H_3^+$ channel has the largest yield among the three dissociation channels and it takes less time to accumulate enough events, we will focus our current study on this channel. The yield of this channel is about 16% of that of the nondissociative channel. The dissociation limit of $CH_3^+ + C_5H_3^+$ is at 24 eV whereas the double-ionization threshold of benzene is 24.65 eV. However, according to previous studies of single-photon ionization [21,23], the direct dissociation of $CH_3^+ + C_5H_3^+$ will not appear until 27.8 eV. This suggests the existence of a large activation barrier for dissociation, and this has been computed to be around 3 eV [21,24]. It is relatively easy to assign the nondissociative dication states to the lowest three electronic states: $^3A_{2g}$, $^1E_{2g}$, and $^1A_{1g}$ [20] because these states have ionization energies below 27.8 eV and thus will not have enough energy to overcome the barrier. All three states arise from losing both electrons from two degenerate highest

occupied molecular orbital (HOMO) orbitals. These states are contained under the first major feature in the benzene double-ionization photoelectron spectrum [19,25] [see Fig. 1(c)]. In a previous single-photon ionization experiment [25], it was observed that the yield of the $^3A_{2g}$ state is much lower. We argue this is also true in NSDI where recollision plays a dominant role. It has been calculated that electron-electron correlation in the process of NSDI would favor the production of singlet states due to the fact that electrons with opposite spins can interact more strongly [13]. Considering the small energy difference between the triplet and the singlet states (0.6 eV), the nondissociative dication states are thus primarily assigned to $^1E_{2g}$ and $^1A_{1g}$. It is unlikely to further differentiate these two states because they are strongly coupled to each other due to a highly distorted nuclear geometry.

The assignment for dissociative benzene dication is more complicated because many more states are energetically allowed. Previous studies suggested the dissociation takes place on singlet states with lowest electronic energy, which indeed has a high barrier [24]. However, as we will see later, the double-ionization dynamics are quite different between dissociative and nondissociative dications, and this suggests that dissociative benzene dications have different electronic origins from $^1E_{2g}$ and $^1A_{1g}$. It is entirely plausible, however, that electronically excited states convert their electronic energy through internal conversion and arrive at $^1E_{2g}$ and $^1A_{1g}$ states with high rovibration excitation, which can then overcome the dissociation barrier. Such a pathway is further supported by the fact that the dissociation appearance energy 27.8 eV is actually above the ionization energy of some excited states, which are contained under the second main feature in the single-photon ionization photoelectron spectrum [Fig. 1(c)] [19]. Three lowest excited states are $^1B_{1g}$, $^1E_{1g}$, and $^1B_{2g}$, which arise from losing one electron from the HOMO and the other from the HOMO-1. The even higher energy states [feature 3 in Fig. 1(c)] are excluded because the ionization energies are at least 2 eV higher (except $^1A_{1u}$, which is at 1.5 eV higher). This is supported by the branching ratio between the dissociative and the nondissociative channels, which have an energy difference about 2 eV, but they have almost an order of magnitude difference in yields. The energy upper bound is the maximum available energy (31 eV) in NSDI, which is estimated to be the sum of the single-ionization potential of benzene (9.2 eV) and the maximum recollision energy (22 eV). Further evidence for ruling out the states between 29.5 and 31 eV was provided by single-photon experiments: the energy-dependent yield curve of $CH_3^+ + C_5H_3^+$ [22] does not indicate additional contributions at energies above 29.5 eV. This suggests the high-energy states do not primarily dissociate with $CH_3^+ + C_5H_3^+$. Triplet states with similar ionization energies are excluded due to the aforementioned exchange-correlation argument and the fact that the dissociation limit leading to triplet state fragments (either CH_3^+ or $C_5H_3^+$) is at least 1 eV higher [26]. It should be noted that the calculated energy difference among $^1B_{1g}$, $^1E_{1g}$, and $^1B_{2g}$ is less than 0.2 eV [20], so energetically it is very difficult to further differentiate these states. See Supplemental Material [27] for a table summarizing the energetics of all low-lying states of benzene dication and the criteria for their qualitative assignment to the dissociative and nondissociative channels.

Now that we have identified major states associated with dissociative and nondissociative benzene dications, we can move to discuss state-resolved NSDI dynamics. In both cases, we observed side-by-side (the first and third quadrants) and back-to-back (the second and fourth quadrants) ejection of electrons parallel to the laser polarization (Fig. 2). However, the major difference lies in the momentum correlation on the plane perpendicular to the laser polarization. Figure 3 shows the electron-momentum correlation on the perpendicular plane for the electrons in coincidence with nondissociative benzene dications. For the side-by-side events along the laser polarization, a clear preference toward 180° for the angle between two

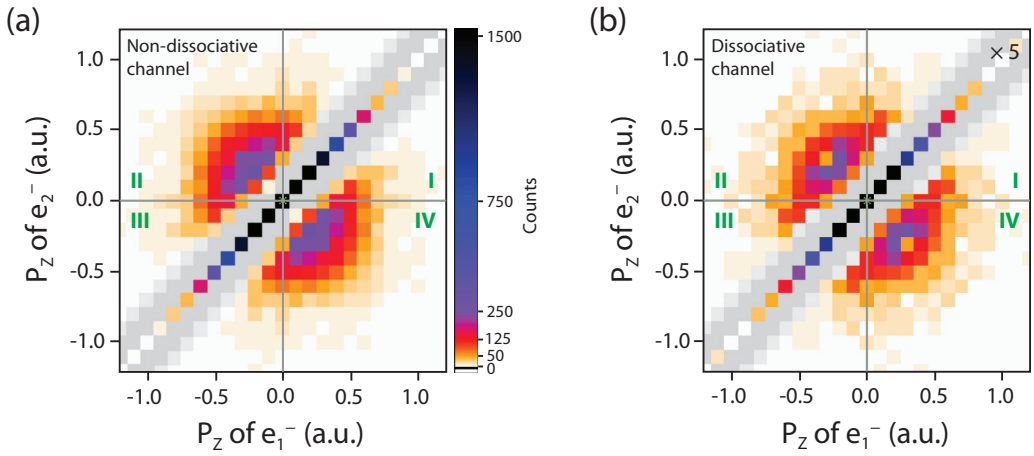

FIG. 2. (a) Electron-momentum correlation parallel to the laser polarization for electrons in coincidence with nondissociative dications. (b) The same as (a) but for electrons in coincidence with dissociative dications. The green roman numbers label the different quadrants. Note the gray area represents the physical dead time of our imaging system (<1 ns) converted to momentum space. The events in this area are not lost but moved to the diagonal line. The magnitude of the momentum of these events will have a small uncertainty. However, the directions of the momentum in the perpendicular plane are completely accurate as determined by a camera, and this provides accurate momentum correlation in the perpendicular plane as shown in Figs. 3 and 4. Therefore, our new imaging system greatly enhances the two-electron coincidence detection efficiency.

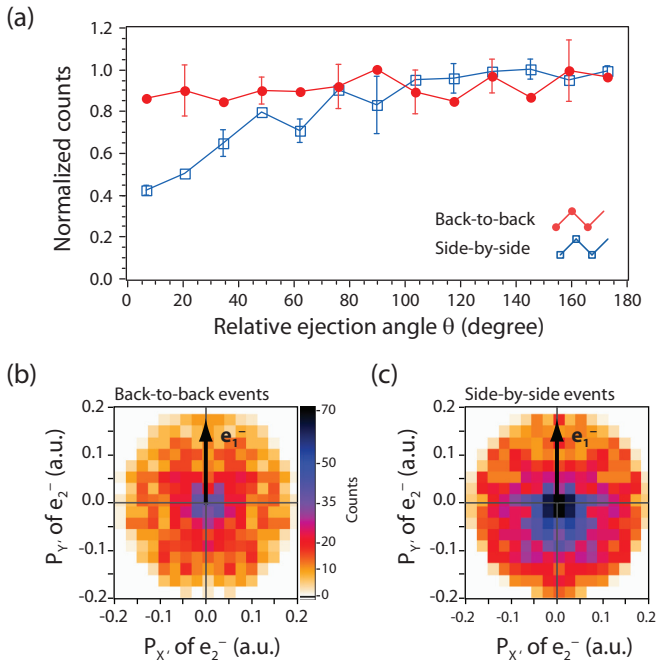

FIG. 3. (a) The normalized electron-pair counts with different relative angles between the momentum vectors on the plane perpendicular to the laser polarization. The electrons are in coincidence with nondissociative $^1E_{2g}$ and $^1A_{1g}$ benzene dication states. Back to back and side by side are defined with respect to the relative ejection direction of two electrons along the laser polarization direction (Z axis). (b) and (c) are the second electron's momentum distributions when aligning the first electron's momentum vector along $+Y'$ direction (X' and Y' are arbitrary axes on the perpendicular plane) for back-to-back and side-by-side events, respectively.

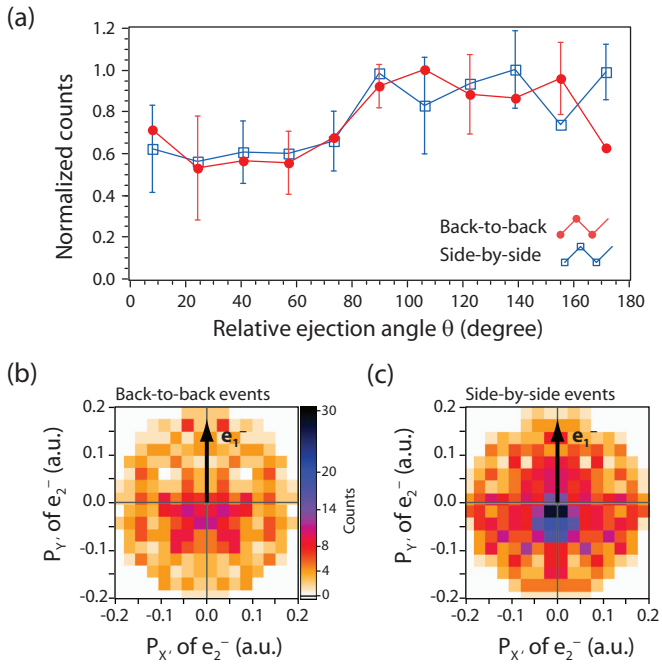

FIG. 4. The same as Fig. 3 but for electrons in coincidence with dissociative dications states, $^1B_{1g}$, $^1E_{1g}$, and $^1B_{2g}$.

electrons' momenta in the perpendicular plane is seen whereas such a preference is absent for back-to-back events. For electrons in coincidence with dissociative dications (Fig. 4), the transverse-momentum correlations show a clear preference toward 180° for both side-by-side and back-to-back events.

For nondissociative benzene dications, the momentum-correlation results are similar to neon at 2×10^{14} W cm^2 [28] and a recent result of argon NSDI at 1.2×10^{14} W cm^2 [29]. Such results have been explained by invoking the presence of doubly excited states after recollision because the energy of the recolliding electron is below the ionization potential of the ions. However, in the current experiment, the maximum recollision energy is $3.17\,U_p \sim 22$ eV and significantly higher than the second ionization energy (~15 eV) leading to $^1E_{2g}$ and $^1A_{1g}$ states (nondissociative). This would enable the RII mechanism, which will account for the side-by-side events. In this mechanism because the electrons are ionized at similar times, they will gain similar momentum from the laser field and emerge as side-by-side events along the laser polarization. When electrons are ionized in the close proximity (time and space) of each other, Coulomb repulsion between electrons will manifest in the magnitude of momentum along the polarization [30,31] or in the relative angle of electron momentum on the perpendicular plane [28]. The strong anticorrelation in the transverse momentum observed for side-by-side events is in a good agreement with this mechanism. However, due to the presence of numerous excited states of benzene neutrals and cations, RESI or doubly excited-state pathways cannot be ruled out completely. These pathways will lead to ionization at different times and thus back-to-back events. When the ionization time is significantly different, the final-state correlation (Coulomb repulsion) is weak or absent. This is also in agreement with the noncorrelated transverse momentum of back-to-back events.

From the above argument, it seems the relative momentum along the polarization direction can be nicely correlated with ionization time difference. However, if we follow this argument, it is indeed surprising to observe strong transverse-momentum correlation in both side-by-side and back-to-back events for the electrons in coincidence with dissociative dications (Fig. 4). In order to manifest a strong momentum correlation in the perpendicular plane for back-to-back events, the condition of close proximity of ionization time has to be met. However this would lead to a similar momentum along the laser polarization, and thus electrons should emerge as side-by-side events instead. A viable mechanism to this seemingly contradictory observation is the presence of a strongly correlated three-body state (electron-electron-ion) and a simultaneous ionization of two electrons near the peak of the laser field when the vector potential is close to zero. Here the Coulomb repulsion between two electrons will lead to momentum anticorrelation in all three dimensions. Such a mechanism has been proposed in a few theoretical works [9,32], and Chen *et al.* [32] further suggested the origin of such an exotic state being electron recapturing by the ion to form a doubly excited state with strong correlation among three bodies. Possible candidates are Rydberg states with ionic cores of $^1B_{1g}$, $^1E_{1g}$, and $^1B_{2g}$. A more interesting

possibility is the formation of a strongly correlated Cooper pair during ionization, which has been recently proposed in benzene single-photon ionization [33]. It should be noted that maximum recollision energy (22 eV) is close to the second ionization energy (∼19 eV) leading to $^1B_{1g}$, $^1E_{1g}$, and $^1B_{2g}$ benzene dication states (dissociative). Although this recollision energy still allows RII mechanism, its relative importance is reduced, and thus other mechanisms could play a more prominent role.

To conclude, with the current coincidence imaging system, we have observed a 3D momentum anticorrelation in electrons arising from double ionization of benzene to $^1B_{1g}$, $^1E_{1g}$, and $^1B_{2g}$ dication states but not to $^1E_{2g}$ and $^1A_{1g}$. Our experimental evidence points to the involvement of strongly correlated doubly excited states, and it will be interesting to see whether theory work can identify these states.

We would like to acknowledge the U.S. Army Research Laboratory and the U.S. Army Research Office for financial support (Awards No. W911NF-12-1-0598 and No. W911NF-14-1-0473). W.L. was partially supported by a fellowship from the Alfred P. Sloan Foundation.

[1] W. Becker, X. Liu, P. J. Ho, and J. H. Eberly, Rev. Mod. Phys. **84**, 1011 (2012).
[2] T. Weber, H. Giessen, M. Weckenbrock *et al.*, Nature (London) **405**, 658 (2000).
[3] B. Feuerstein, R. Moshammer, D. Fischer *et al.*, Phys. Rev. Lett. **87**, 043003 (2001).
[4] E. Eremina, X. Liu, H. Rottke *et al.*, J. Phys. B: At., Mol. Opt. Phys. **36**, 3269 (2003).
[5] M. Weckenbrock, A. Becker, A. Staudte, S. Kammer, M. Smolarski, V. R. Bhardwaj, D. M. Rayner, D. M. Villeneuve, P. B. Corkum, and R. Dörner, Phys. Rev. Lett. **91**, 123004 (2003).
[6] Y. Liu, D. Ye, J. Liu *et al.*, Phys. Rev. Lett. **104**, 173002 (2010).
[7] B. Bergues, M. Kübel, N. G. Johnson *et al.*, Nat. Commun. **3**, 813 (2012).
[8] P. B. Corkum, Phys. Rev. Lett. **71**, 1994 (1993).
[9] A. Emmanouilidou, Phys. Rev. A **83**, 023403 (2011).
[10] T. Brabec, M. Y. Ivanov, and P. B. Corkum, Phys. Rev. A **54**, R2551 (1996).
[11] E. Eremina, X. Liu, H. Rottke, W. Sandner, M. G. Schätzel, A. Dreischuh, G. G. Paulus, H. Walther, R. Moshammer, and J. Ullrich, Phys. Rev. Lett. **92**, 173001 (2004).
[12] D. Zeidler, A. Staudte, A. B. Bardon, D. M. Villeneuve, R. Dörner, and P. B. Corkum, Phys. Rev. Lett. **95**, 203003 (2005).
[13] C. Ruiz, L. Plaja, and L. Roso, Laser Phys. **16**, 600 (2006).
[14] S. G. Sayres, E. R. Hosler, and S. R. Leone, J. Phys. Chem. A **118**, 8614 (2014).
[15] S. K. Lee, F. Cudry, Y. F. Lin *et al.*, Rev. Sci. Instrum. **85**, 123303 (2014).
[16] S. K. Lee, Y. F. Lin, S. Lingenfelter *et al.*, J. Chem. Phys. **141**, 221101 (2014).
[17] Y. F. Lin, S. K. Lee, P. Adhikari *et al.*, Rev. Sci. Instrum. **86**, 096110 (2015).
[18] S. M. Sharifi, A. Talebpour, and S. L. Chin, J. Phys. B: At., Mol. Opt. Phys. **40**, F259 (2007).
[19] K. Jänkälä, P. Lablanquie, F. Penent, J. Palaudoux, L. Andric, and M. Huttula, Phys. Rev. Lett. **112**, 143005 (2014).
[20] F. Tarantelli, A. Sgamellotti, L. S. Cederbaum *et al.*, J. Chem. Phys. **86**, 2201 (1987).
[21] M. Alagia, P. Candori, S. Falcinelli *et al.*, J. Chem. Phys. **135**, 144304 (2011).
[22] M. Alagia, P. Candori, S. Falcinelli *et al.*, Phys. Chem. Chem. Phys. **13**, 8245 (2011).
[23] A. E. Slattery (http://www.starscape.org.uk/thesis/aeslattery04_chapter5.pdf).
[24] S. Anand and H. B. Schlegel, J. Phys. Chem. A **109**, 11551 (2005).
[25] J. H. D. Eland, Chem. Phys. **345**, 82 (2008).
[26] B. Weiner, C. J. Williams, D. Heaney *et al.*, J. Phys. Chem. **94**, 7001 (1990).
[27] See Supplemental Material at http://link.aps.org/supplemental/10.1103/PhysRevA.93.031402 for a table summarizing the energetics of benzene dication and criteria for state assignment.
[28] M. Weckenbrock, D. Zeidler, A. Staudte *et al.*, Phys. Rev. Lett. **92**, 213002 (2004).
[29] Q. Liao, A. H. Winney, S. K. Lee *et al.* (unpublished).
[30] A. Rudenko, V. L. B. de Jesus, T. Ergler, K. Zrost, B. Feuerstein, C. D. Schröter, R. Moshammer, and J. Ullrich, Phys. Rev. Lett. **99**, 263003 (2007).
[31] A. Staudte, C. Ruiz, M. Schöffler, S. Schössler, D. Zeidler, T. Weber, M. Meckel, D. M. Villeneuve, P. B. Corkum, A. Becker, and R. Dörner, Phys. Rev. Lett. **99**, 263002 (2007).
[32] Z. Chen, Y. Liang, D. H. Madison, and C. D. Lin, Phys. Rev. A **84**, 023414 (2011).
[33] R. Wehlitz, P. N. Juranić, K. Collins, B. Reilly, E. Makoutz, T. Hartman, N. Appathurai, and S. B. Whitfield, Phys. Rev. Lett. **109**, 193001 (2012).